



# Temperature and Redox-Responsive Hydrogels Based on Nitroxide Radicals and Oligoethyleneglycol Methacrylate

Miriam Khodeir, Sayed Antoun, Evelyne van Ruymbeke, and Jean-François Gohy\*

A temperature and redox-responsive polymer hydrogel is constructed by randomly incorporating 2,2,6,6-tetramethyl-1-piperidinyloxy-methacrylate (TEMPO) stable nitroxide radicals and oligoethyleneglycol methacrylate (OEGMA) groups in a polymer network. TEMPO can be reversibly oxidized into an oxoammonium cation (TEMPO<sup>+</sup>) providing the redox-responsive properties while the lower critical solubility temperature (LCST) of OEGMA results in temperature-responsive properties. Since a rather low amount of di(ethylene glycol) dimethacrylate (OEGMA<sub>2</sub>) is used to chemically cross-link the polymer network, the accordingly formed hydrogels obtained after swelling with water consist of microgel particles with entangled polymer chains that are not chemically crosslinked. By varying the amount of TEMPO in the polymer network, it is demonstrated that the radical form of TEMPO aggregates into hydrophobic domains acting as physical crosslinking nodes in the hydrogels and further increasing the cohesion between microgel particles. Increasing the temperature results in two opposite effects on the solubility of TEMPO and OEGMA units. The oxidation of TEMPO into TEMPO<sup>+</sup> also results in a deep change in the hydrogel properties since TEMPO<sup>+</sup> units are essentially hydrophilic and do not aggregate into physical crosslinking nodes.

## 1. Introduction

Over the past century, hydrogels have emerged as effective materials for an immense variety of applications.<sup>[1]</sup> Hydrogels are water-swollen polymeric materials that maintain their 3D structure. Stimuli-responsive hydrogels also called “smart” materials have diverse potential applications<sup>[2]</sup> in the field of drug delivery, tissue engineering, agriculture, cosmetics, gene therapy, and as sensors and actuators due to their unique

responsiveness to internal and/or external chemophysical stimuli, such as pH,<sup>[3]</sup> temperature,<sup>[4]</sup> and ionic strength.<sup>[5]</sup> Understanding the responsiveness of hydrogel structure and rheological properties to these stimuli is essential for designing materials with desirable performance.

Among the previously investigated stimuli, few studies have focused on redox-responsive hydrogels. As typical examples, multistimuli responsive hydrogels based on ferrocene, a redox-active group, have been reported by several groups. In this respect, Zhang and co-workers fabricated ferrocenyl phenylalanine supramolecular hydrogels exhibiting a sharp phase transition in response to redox potential.<sup>[6]</sup> In another work, Wang and co-workers<sup>[7]</sup> described the fabrication of self-healing and multistimuli responsive hydrogels using the self-assembly of biodegradable ferrocene-modified chitosan in an acid aqueous solution at a low concentration of 10 mg mL<sup>-1</sup>.<sup>[7]</sup> It was shown that the resulting hydrogels possessed excellent redox, pH and ion responsiveness.<sup>[7]</sup> More-

over, the redox stimulus has been rarely combined with temperature-responsive behavior. Among the few works performed in this direction, the results obtained by Zheng and co-workers<sup>[8]</sup> can be cited here, where thermo- and redox-responsive hydrogels based on copolymers of *N*-isopropylacrylamide (NIPAM) and an ionic liquid-containing monomer were synthesized.<sup>[8]</sup> Those hydrogels presented a high thermoresponsive sensitivity and good redox-responsiveness originating from the transition of iron ions between two oxidation states in the gel matrix and making them very interesting candidates for stimuli-responsive electronic devices or other self-adaptive electronics.<sup>[8]</sup> In another example, a dual redox- and thermoresponsive hydrogel was synthesized based on NIPAM and ferrocenyl silane-vinyl imidazolium (FS-Vim) ionic liquid monomers.<sup>[9]</sup> In this system, the FS-Vim poly(ionic liquid) was used as macrocrosslinker and provided redox-responsive properties to the system while the lower critical transition temperature (LCST) of poly(NIPAM) was influenced by the incorporation of the poly(ionic liquid). Moreover the swelling ability and thermoresponsivity of those hydrogels could be tuned by the counterions associated with the poly(ionic liquid) part.

The present contribution is focused on the understanding of the relationships between structure-properties of redox and temperature responsive hydrogels essentially through the study

M. Khodeir, Prof. E. van Ruymbeke, Prof. J.-F. Gohy  
Institute of Condensed Matter and Nanosciences (IMCN)  
Bio and Soft Matter (BSMA)  
Université catholique de Louvain (UCL)  
Place L. Pasteur 1 & Croix du Sud 1, B-1348 Louvain-la-Neuve, Belgium  
E-mail: jean-francois.gohy@uclouvain.be  
Prof. S. Antoun  
Department of Chemistry  
Faculty of Science Section III- North Campus-Tripoli  
Lebanese University (UL)  
Lebanon

The ORCID identification number(s) for the author(s) of this article can be found under <https://doi.org/10.1002/macp.201900550>.

DOI: 10.1002/macp.201900550

of their rheological properties. The knowledge of such properties is fundamental because, on one hand, these properties can help us to decipher the hydrogel structure on the micrometer scale and, on the other hand, the gained knowledge allows the modulation and optimization of the hydrogel properties for application in different fields. More precisely, we evaluate in the present paper the mechanical properties of redox and temperature responsive hydrogels by standard mechanical testing methods such as elastic or storage modulus ( $G'$ ) and viscous or loss modulus ( $G''$ ) measurements, through dynamic mechanical tests at different deformation amplitudes. All rheological properties are evaluated through the use of rotational rheometers. To this aim, we design redox and temperature responsive hydrogels that contain the 2,2,6,6-tetramethyl-1-piperidinyloxy (TEMPO) groups as redox-active components. TEMPO is a stable nitroxide radical that can be easily oxidized into its oxoammonium counterpart or reduced into an aminoxyl group.<sup>[10]</sup> The water solubility is provided by the presence of the thermoresponsive (oligoethyleneglycol)methacrylate (OEGMA) comonomer. Here, we have selected an OEGMA monomer containing 4/5 ethylene glycol units and displaying a cloud-point of 65 °C. As stated above, the combination of redox and temperature-responsive behaviors in a same hydrogel has been rarely studied. Moreover, since the redox process utilized in this contribution results in the transformation of TEMPO, which essentially behave as an hydrophobic unit, into oxidized TEMPO (TEMPO<sup>+</sup>) which is hydrophilic, an interplay between the redox and temperature behaviors is expected because the cloud point of polymers is known to be influenced by either the presence of neighboring hydrophobic or hydrophilic units.<sup>[11]</sup>

In a previous very recent study on this system, we have focused on the effects of the covalent crosslinking degree and of the content of TEMPO units on the properties of the hydrogels at room temperature.<sup>[12]</sup> We have demonstrated that the optimum molar fraction of crosslinker,  $X_{CL}$ , is equal to 0.03 in order to obtain homogeneous gels displaying high swelling ratios. By varying the amount of TEMPO units (expressed as  $X_{TEMPO}$  molar fraction) in the hydrogels, we have confirmed that our hydrogels are slightly chemically crosslinked systems further reinforced by physically crosslinked nanodomains resulting from the aggregation of hydrophobic TEMPO units.<sup>[12]</sup> Here, our aim is to decipher the effects of temperature and redox stimuli on the rheological properties of reduced P(TEMPO-*r*-OEGMA) and oxidized P(TEMPO<sup>+</sup>-*r*-OEGMA) hydrogels with varying TEMPO content at a fixed covalent crosslinking degree.

## 2. Results and Discussion

### 2.1. Synthesis and Characterization of P(TEMPO-*r*-OEGMA) and P(TEMPO<sup>+</sup>-*r*-OEGMA) Hydrogels

P(TEMPO-*r*-OEGMA) hydrogels with different  $X_{TEMPO}$  and  $X_{CL}$  equal to 0.03 (Figure 1) were synthesized using the same experimental protocol as described in our previous report.<sup>[12]</sup>  $X_{CL}$  was set to 0.03 since the accordingly obtained hydrogels present the highest swelling factor (defined as  $[(W_s - W_d)/W_d]$  where  $W_s$  is the weight of the hydrogel in the swollen state at equilibrium

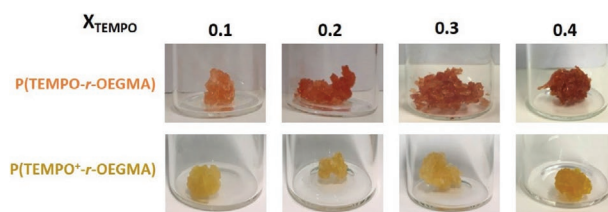


**Figure 1.** Library of the reduced P(TEMPO-*r*-OEGMA) and oxidized P(TEMPO<sup>+</sup>-*r*-OEGMA) hydrogels with  $X_{CL} = 0.03$  and various  $X_{TEMPO}$ .

and  $W_d$  is the weight of the hydrogel in the dry state) with a value around 35 (meaning that 0.025 g of gel absorb 1 g of water) for a P(TEMPO-*r*-OEGMA) hydrogel with  $X_{TEMPO} = 0.2$ . Lower  $X_{CL}$  eventually leads to viscous fluids instead of gels (Table S1, Supporting Information) and lower swelling factors are observed for higher  $X_{CL}$ . Those results can be easily understood considering that the increase of crosslinker ratio leads to a decrease of the capacity of the 3D polymer network to retain water due to the decrease in the mesh size of the network.

The P(TEMPO-*r*-OEGMA) hydrogels were converted into P(TEMPO<sup>+</sup>-*r*-OEGMA) ones by the chemical oxidation of the nitroxide radicals into oxoammonium cations using NaClO. This reaction can be visually monitored by the change of color of the hydrogel from orange to yellow (Figure 1). The UV-vis spectra of P(TEMPO-*r*-OEGMA) and P(TEMPO<sup>+</sup>-*r*-OEGMA) are shown in Figure S1 (Supporting Information). FTIR spectroscopy (Figure S2, Supporting Information) also confirms the oxidation of P(TEMPO-*r*-OEGMA) (with a characteristic N–O vibration at 1540 cm<sup>−1</sup>) into P(TEMPO<sup>+</sup>-*r*-OEGMA) (with a characteristic N=O vibration at 1570 cm<sup>−1</sup>). The yield of this reaction was determined to be close to 100% in our previous work by using electron spin resonance.<sup>[12]</sup> Furthermore, cyclic voltammetry measurements confirmed the presence of redox responsive TEMPO groups in our materials and the reversibility of the redox reactions.<sup>[12]</sup>

In order to get some additional information about the structure of the gel, soluble fractions of the investigated hydrogels have been extracted and further analyzed by dynamic light scattering (DLS). Indeed, as demonstrated in our previous report,<sup>[12]</sup> our hydrogels are slightly chemically crosslinked and therefore contain a significant fraction of free or slightly crosslinked chains that can be extracted from the equilibrated hydrogels by bringing them into contact in an aqueous phase. In our previous report, the fraction of extracted was further quantified by <sup>1</sup>H NMR using an internal standard.<sup>[12]</sup> Cryotransmission electron microscopy experiments were also realized on the diluted hydrogels in order to visualize the hydrophobic nanodomains and their distribution in the hydrogel. Unfortunately, it was not possible to obtain interesting information from those experiments.<sup>[12]</sup> Here, we have carried out DLS experiments in order to get more information about the structure of the extracted species. In this respect, objects with a mean hydrodynamic radius of 23 nm have been detected by DLS (Figure S3, Supporting Information). This can be again explained by the fact that our hydrogels are not consisting of a single macroscopic network of crosslinked polymers but are rather cluster of smaller hydrogel particles linked together by entangled noncrosslinked polymer chains and/or hydrophobic TEMPO domains.

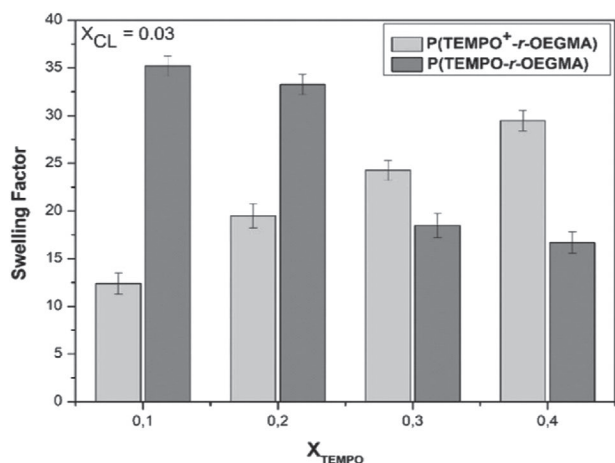


**Figure 2.** The swelling factors at room temperature for the reduced P(TEMPO-r-OEGMA) and oxidized P(TEMPO<sup>+</sup>-r-OEGMA) hydrogels with different  $X_{\text{TEMPO}}$  and fixed  $X_{\text{CL}} = 0.03$ . Error bars represent average swelling ratio  $\pm$  standard deviation where  $n = 3$ .

## 2.2. Mechanical Characterization

### 2.2.1. Swelling Tests

Swelling tests were performed on the P(TEMPO-r-OEGMA) and P(TEMPO<sup>+</sup>-r-OEGMA) hydrogels. The swelling factor was measured for all  $X_{\text{TEMPO}}$  values with  $X_{\text{CL}}$  equal to 0.03. The equilibrium state was determined by regularly weighting the hydrogel during the swelling process until it reached a constant weight. This was typically achieved after 24 h (Figure S4, Supporting Information). However, in order to be sure to be at the equilibrium, the hydrogels were further equilibrated for a total of 48 or 72 h before measuring them again. P(TEMPO<sup>+</sup>-r-OEGMA) hydrogels with varying  $X_{\text{TEMPO}}$  ratio and  $X_{\text{CL}}$  fixed to 0.03 display swelling factors around 12–18 for  $X_{\text{TEMPO}}$  of 0.1 and 0.2 (Figure 2) while for  $X_{\text{TEMPO}}$  of 0.3 and 0.4, the swelling factors increase by nearly a factor of 1.4. This increase of swelling factors with the content of  $X_{\text{TEMPO}}$  can be explained by

the increase in hydrophilicity provided by the TEMPO<sup>+</sup> units. Indeed, P(TEMPO-r-OEGMA) hydrogels with varying  $X_{\text{TEMPO}}$  and  $X_{\text{CL}}$  fixed to 0.03 display an opposite effect (Figure 2). In this case, the swelling factors decrease by nearly a factor of two when the amount of TEMPO units is increased ( $X_{\text{TEMPO}}$  of 0.3 and 0.4), which can be explained by the increase in hydrophobicity provided by the TEMPO units. Furthermore, increasing the TEMPO units leads to electrostatic repulsion along the chains, which could favor their swelling.

Interestingly enough, the swelling factors of the reduced P(TEMPO-r-OEGMA) hydrogels are much higher than the swelling factors of the P(TEMPO<sup>+</sup>-r-OEGMA) ones at low TEMPO content. This observation might be a bit surprising since one could expect higher swelling factors for more hydrophilic P(TEMPO<sup>+</sup>-r-OEGMA) hydrogels. One should however remind that the swelling factor is measuring the ability of the hydrogels to absorb water while keeping its structure. In that respect, the presence of physically crosslinking nodes arising from the aggregation of TEMPO units into small hydrophobic domains could increase the average size of the clusters and their capacity to absorb and retain water in the hydrophilic regions. Such a situation will not be observed for the fully hydrophilic P(TEMPO<sup>+</sup>-r-OEGMA) hydrogels in which only chemical crosslinks are present. The following results will give credit to this hypothesis of formation of hydrophobic TEMPO domains.

The temperature-dependent swelling profiles of the P(TEMPO-r-OEGMA) and P(TEMPO<sup>+</sup>-r-OEGMA) hydrogels with varying amounts of TEMPO units and  $X_{\text{CL}}$  equal to 0.03 are shown in Figure 3. In both cases, as temperature increases, the swelling factors decrease. The influence of temperature is complex to interpret since different effects are expected to come into play. For the P(TEMPO<sup>+</sup>-r-OEGMA) hydrogels, the hydrophilic TEMPO<sup>+</sup> units are not expected to be influenced by temperature. In sharp contrast, OEGMA units are known to display a cloud-point in water due to the breaking of the hydrogen bonds between ether oxygens in OEGMA and water molecules as temperatures increases. The cloud-point of the OEGMA used here is reported to be located at 65 °C.<sup>[13]</sup> Thus, the

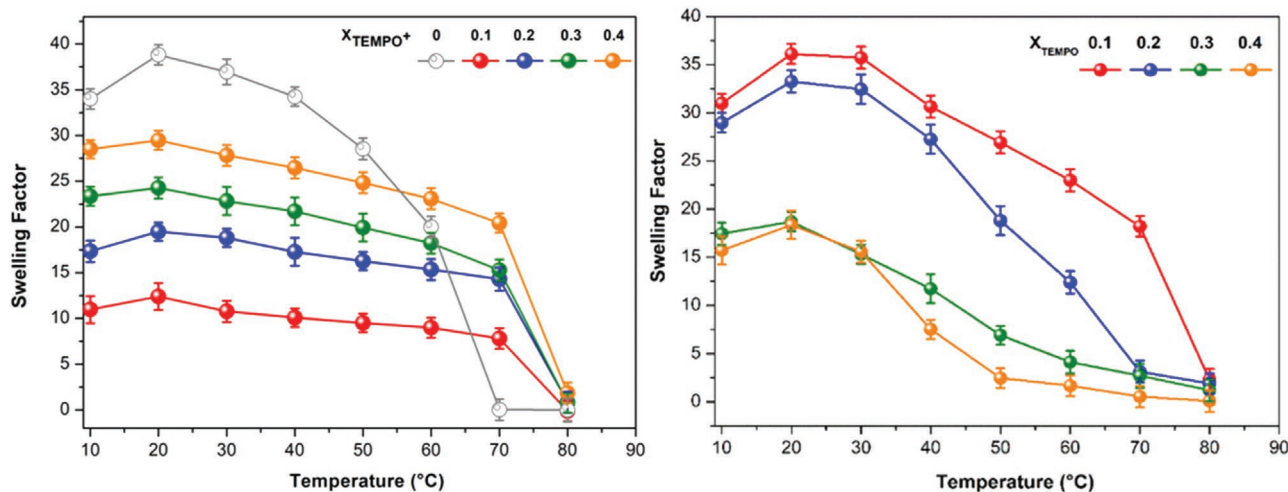


**Figure 3.** Temperature-dependent swelling profiles of P(TEMPO<sup>+</sup>-r-OEGMA) (left) and P(TEMPO-r-OEGMA) (right) hydrogels for different  $X_{\text{TEMPO}}$  and  $X_{\text{CL}} = 0.03$ . Error bars represent average swelling ratio  $\pm$  standard deviation where  $n = 3$ .

hydrogel should collapse and become macroscopically turbid once the cloud-point is reached. This could ultimately lead to a macrophase separation between a collapsed gel and an aqueous phase. However, the value of the cloud-point could be influenced by neighboring hydrophilic/hydrophobic groups.<sup>[11,14]</sup> Generally, hydrophobic groups lower the cloud-point while hydrophilic groups shift the cloud-point toward higher temperature.<sup>[15]</sup> In Figure 3, one can observe that, whatever the value of  $X_{\text{TEMPO}}^+$ , the swelling factors values are slightly decreasing as temperature increases and dramatically drop down between 70 and 80 °C. One can conclude that the cloud points of the P(TEMPO<sup>+</sup>-*r*-OEGMA) hydrogels are located in this temperature range and slightly shifted to higher temperature compared to pure OEGMA due to the presence of hydrophilic TEMPO<sup>+</sup> units as shown in Figure 3.

In the case of the P(TEMPO-*r*-OEGMA) hydrogels, the hydrophobic TEMPO units are expected to lower the cloud-point of OEGMA. In this respect, the swelling factor drops down to a value close to 0 at temperatures below 65 °C for the P(TEMPO-*r*-OEGMA) with  $X_{\text{TEMPO}}$  of 0.4 and 0.3, around 65 °C for  $X_{\text{TEMPO}}$  of 0.2 and close to 80 °C for the lowest value of  $X_{\text{TEMPO}}$  (0.1) (Figure 3). To understand those values, it should be noted that an increase in temperature is known to increase the solubility of TEMPO units. Indeed, TEMPO-methacrylate polymers are known to exhibit LCST behavior in water-containing solvents,<sup>[16]</sup> and thus to lead to the weakening or disintegration of hydrophobic TEMPO-rich domains. Thus, the two hypothesized effects are going in opposite directions: on one hand hydrophobic TEMPO units should decrease the cloud point of OEGMA (this effect is essentially observed for the hydrogels containing the highest amount of TEMPO, i.e., 0.4) and, on the other hand, TEMPO units start to be hydrophilic at higher temperature (this effect is essentially observed for the hydrogels containing the lowest amount of TEMPO, i.e., 0.1). For  $X_{\text{TEMPO}}$  values of 0.2 and 0.3, an intermediate behavior between the two extreme is observed. Those combined two effects could explain the evolution observed in Figure 3 for the swelling factors of P(TEMPO-*r*-OEGMA) hydrogels as temperatures increases.

### 2.2.2. Rheological Characterization

The viscoelastic properties of the P(TEMPO-*r*-OEGMA) hydrogels were investigated by rotational rheometry. The viscoelastic response was first measured as a function of temperature for the reference hydrogel without TEMPO units and for the ones with  $X_{\text{TEMPO}}$  values equal to 0.1 and 0.4. As shown in Figure 4, the storage modulus ( $G'$ ) decreases when the temperature increases, while it increases when the value of  $X_{\text{TEMPO}}$  increases. The effect of  $X_{\text{TEMPO}}$  can be understood on the basis of the formation of hydrophobic TEMPO-rich domains acting as physical crosslinking nodes in the hydrogel. Those ones are added to the chemical crosslinking nodes afforded by OEGMA<sub>2</sub> units and are basically acting as mechanically reinforcing nodes, resulting in a higher  $G'$ . This effect is more pronounced as the content of TEMPO is increased in the hydrogels resulting in more or larger hydrophobic domains.

The effect of temperature has to be discussed with an approach similar to the one used for explaining the evolution

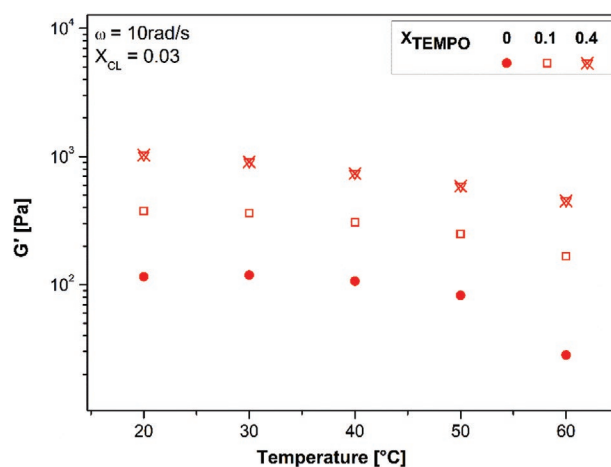


**Figure 4.** Temperature-dependent of elastic modulus  $G'$  behavior of the hydrogel reference without TEMPO and for the P(TEMPO-*r*-OEGMA) hydrogels with the lowest and highest  $X_{\text{TEMPO}}$  values 0.1 and 0.4 respectively with  $X_{\text{CL}}$  0.03.

of the swelling factor as a function of temperature. On the one hand, higher temperature increases the solubility of TEMPO that could ultimately lead to the disappearance of the TEMPO physical crosslinks within and between the hydrogel particles. On the other hand, the solubility of the OEGMA decreases with increasing the temperature and OEGMA becomes insoluble once its cloud point is reached. As already discussed, the value of the OEGMA cloud point might vary with the composition of the hydrogel since it is likely influenced by the TEMPO units (in a rather complex way since the hydrophilic/hydrophobic character of TEMPO units also varies with temperature). Once the cloud point of OEGMA is reached, the hydrogel should collapse and become macroscopically turbid. This could ultimately lead to a macrophase separation between a collapsed gel and an aqueous phase. This situation has been observed for our gels at high temperature (above 60 °C) in line with the swelling factors measurements (in this case swelling factors of 0 have been measured). Due to the formation of heterogeneous systems composed of a flowing liquid and a solid phase, rheological measurements could not be performed above 60 °C. Below this temperature, as expected, the storage moduli of the investigated gels were found to decrease as temperature increases (Figure 4).

In order to investigate the reversible behavior of our hydrogels, strain sweep tests have been performed from low to high strain amplitude and then, from high to low strain. Results are shown in Figure 5 for  $X_{\text{TEMPO}} = 0$  (left) and for  $X_{\text{TEMPO}} = 0.1$  and 0.4 (right). In the case of the hydrogel with no TEMPO unit (Figure 5, left), a hysteresis is observed, which confirms the formation of hydrogels consisting of clusters of smaller hydrogel particles able to deform and held together via hydrogen bonds between OEGMA units and water molecules.

For the two samples containing TEMPO units, a hysteresis is also observed, which can be seen as a signature of reversible bonds. High strain leads to partial breaking of the hydrophobic interactions between TEMPO units, to allow the hydrogel particles to deform and adapt to the flow. When coming back to low strain amplitude, these interactions are formed again, and the initial value of the modulus is recovered. By increasing the



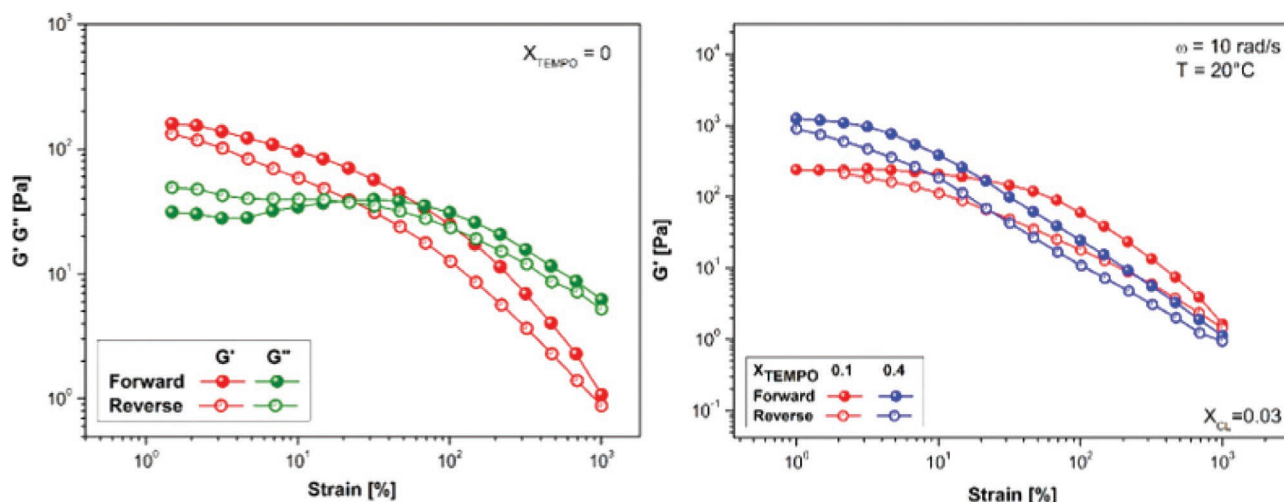


**Figure 5.** (Left) Storage and loss modulus of the hydrogel without TEMPO units  $X_{CL} = 0.03$ . (Right) Storage modulus of the hydrogels with the lowest amount of TEMPO units (0.1, red curve) and the highest amount (0.4, blue curve) with  $X_{CL} = 0.03$ . From low to high (filled symbols) or high to low (empty symbols) amplitude of deformation.

amount of TEMPO units from 0.1 to 0.4, hydrophobic interactions are promoted, which leads to a higher modulus at low strain amplitude but also, to a shorter linear regime.

These results are also in line with the structure of our hydrogels that are poorly crosslinked and rather consist of clusters of hydrogel particles held together by TEMPO-rich domains (hydrophobic interactions) and entangled free polymer chains.

Regarding the oxidized P(TEMPO<sup>+</sup>-r-OEGMA) hydrogels, frequency sweeps were first performed to confirm gel formation (Figure 6, left). While comparing the rheological properties of the P(TEMPO-r-OEGMA) and P(TEMPO<sup>+</sup>-r-OEGMA) hydrogels (Figure 6, left), the storage modulus of the charged gels decreases when the amount of TEMPO<sup>+</sup> units increases, in sharp contrast with the noncharged gels where  $G'$  increases when the amount of TEMPO units increases. This behavior can be explained by the lack of hydrophobic TEMPO units acting as mechanically-reinforcing physical crosslinks in the case of P(TEMPO<sup>+</sup>-r-OEGMA) hydrogels.

Moreover, increasing the amount of TEMPO<sup>+</sup> units increases electrostatic repulsions in the system and therefore, the

attractive interactions between hydrogel particles should vanish at the expense of repulsive ones. In turn, the macroscopic modulus of the hydrogels is expected to decrease as the amount of TEMPO<sup>+</sup> units increases in agreement with the situation observed in Figure 6, left. Frequency sweep measurements were also realized as a function of temperature for the charged P(TEMPO<sup>+</sup>-r-OEGMA) hydrogels in comparison to the reference hydrogel with no TEMPO (Figure 6, right). The evolution of  $G'$  as a function of temperature is similar to the one noted previously of the uncharged P(TEMPO-r-OEGMA) hydrogels. Since hydrophobic TEMPO domains are not existing in case of the P(TEMPO<sup>+</sup>-r-OEGMA) hydrogels, one can hypothesize that the major effect playing here is the desolvation of OEGMA upon heating. As far as the structural features of the hydrogels are concerned, one can understand that desolvation of OEGMA units will reduce the interactions between the hydrogel particles and the number of hydrogen bonds connecting them, which will lead to lower values of storage modulus.

Finally, strain sweeps tests have also been performed for the P(TEMPO<sup>+</sup>-r-OEGMA) hydrogels from low to high strain

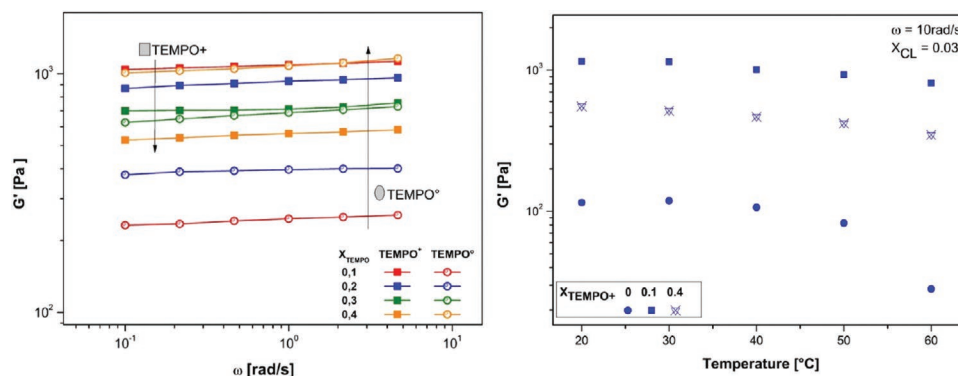


**Figure 6.** (Left) Frequency sweep plots of storage moduli versus frequency for P(TEMPO-r-OEGMA) and P(TEMPO<sup>+</sup>-r-OEGMA) hydrogels with  $X_{CL} = 0.03$ . (Right) Temperature-dependent of elastic modulus  $G'$  behavior of the hydrogel reference without TEMPO and for the P(TEMPO<sup>+</sup>-r-OEGMA) hydrogels with the lowest and highest  $X_{TEMPO+}$  values of 0.1 and 0.4 respectively.

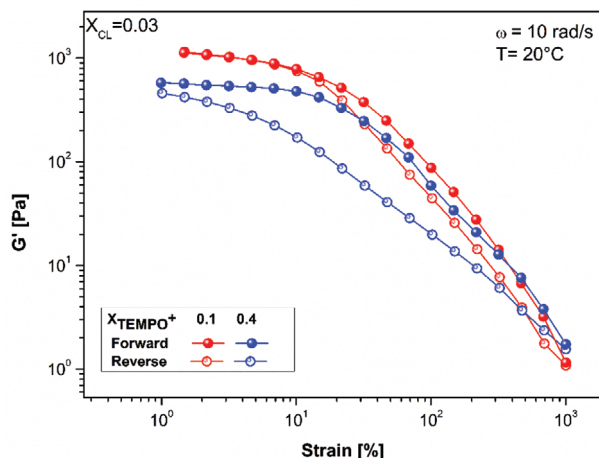


**Figure 7.** Storage modulus of the hydrogels with the lowest amount of TEMPO units (0.1, red curve) and the highest amount (0.4, blue curve) with  $X_{CL} = 0.03$ . From low to high (filled symbols) or high to low (empty symbols) amplitude of deformation.

amplitude and then, from high to low strain. Results are shown in **Figure 7** for  $X_{TEMPO+} = 0.1$  and 0.4. For both samples, a hysteresis is observed, which can be seen as a signature of the deformability of the hydrogel particles and of the reversible bonds (only hydrogen bonds between OEGMA and the water molecule in this case). These results confirm again that our hydrogels are consisting of clusters of smaller hydrogel particles held together by noncovalent interactions.

### 3. Conclusions

This work described the combination of redox and temperature-responsive behaviors in a same hydrogel, which has been rarely studied. As responsive groups, we selected OEGMA with a lower critical solubility temperature (LCST) resulting in temperature-responsive properties and TEMPO radicals as redox-responsive units.

The strategy of synthesis was based on the use of a low amount of difunctional monomer (OEGMA<sub>2</sub>) to chemically crosslink the polymer network.<sup>[12]</sup> Therefore, the accordingly formed hydrogels obtained after swelling with water rather consisted of microgel particles with entangled polymer chains that are not chemically crosslinked, than a continuous polymer network swollen with water. On the basis of the rarely reported approaches on redox-responsive hydrogels,<sup>[17,18]</sup> this work has demonstrated that the TEMPO units in their radical form aggregate into hydrophobic domains acting as physical crosslinking nodes in our hydrogels. Increasing the temperature resulted in two opposite effects. On the one hand, the water solubility of TEMPO units increases as temperature increases resulting in the progressive swelling of the TEMPO domains. On the other hand, the solubility of the OEGMA groups decreases as temperature increases due to their dehydration. The oxidation of TEMPO into TEMPO<sup>+</sup> also resulted in a deep change in the hydrogel properties since TEMPO<sup>+</sup> units are essentially hydrophilic and do not aggregate into physical crosslinking nodes, thus resulting into hydrogels with weaker

mechanical properties than TEMPO-containing hydrogels and with a degree of swelling increasing with the increasing content of TEMPO<sup>+</sup>.

In conclusion, the effects of temperature and redox stimuli on the rheological properties of reduced P(TEMPO-*r*-OEGMA) and oxidized P(TEMPO<sup>+</sup>-*r*-OEGMA) hydrogels with varying TEMPO content at a fixed covalent crosslinking degree have been disclosed in this paper. In our future work, we will detail the concept of the encapsulation/release of a guest molecule from those hydrogels via an electrochemical oxidation of TEMPO group.

### 4. Experimental Section

**Materials and Chemicals:** All chemicals and monomers were purchased from Aldrich, Fluka, or Acros. Solvents were bought from Acros. 2,2,6,6-tetramethyl-1-piperidyl methacrylate (TMPPM), oligo(ethylene glycol) methyl ether methacrylate (OEGMA, average molar mass of 300 g mol<sup>-1</sup>, Aldrich) and di(ethylene glycol) dimethacrylate (OEGMA<sub>2</sub>, Aldrich) were purified on a AlO<sub>x</sub>-filtration column prior use in order to remove the inhibitor. The 2,2'-azobisisobutyronitrile (AIBN, 98% purity, Fluka) initiator was recrystallized twice from methanol prior use.

**Rheological Measurements:** Rheology experiments were performed on a Kinexus Ultra (Malvern Instruments) rheometer equipped with a heat exchanger and modified with a solvent trap. Measurements were carried out using a plate-plate steel geometry (8 and 20 mm diameter plate-plate geometries). Oscillatory measurements were carried out in the linear regime (by imposing either at strain amplitude of 1% or at stress amplitude of 5 Pa) with a gap adjusted between 450 and 1800 μm at given temperatures. A strain sweep test was performed with each sample, to determine the linear viscoelastic (LVE) range. Frequency sweep was then used to determine the storage modulus,  $G'$ , and the loss modulus,  $G''$ , as a function of angular frequency,  $\omega$ . Normal forces were checked to be relaxed prior any measurement.

**Swelling Tests:** The dry gels were swollen in distilled water at 25 °C in an isothermal water bath to study the equilibrium swelling kinetics. Mass measurements were taken at time points of 0, 0.5, 1, 2, 4, 8, 24, 48, 72 h. The swelling factor was defined as the weight ratio between the difference in hydrogel weight in both the dry and the swollen state over the weight of the dry gel. In order to perform a temperature swelling study, gels were swelled at temperature increments of 10 °C from 10 to 80 °C for 24 h to reach equilibrium swelling, and mass swelling ratios at each temperature were calculated.

**Typical Procedure for the Synthesis of P(TEMPO-*r*-OEGMA) and P(TEMPO<sup>+</sup>-*r*-OEGMA) Hydrogels:** The investigated P(TEMPO-*r*-OEGMA) and P(TEMPO<sup>+</sup>-*r*-OEGMA) hydrogels have been synthesized via a methodology described in our previous work.<sup>[12]</sup> Briefly, a P(TMPPM-*r*-OEGMA) precursor hydrogel was prepared by conventional radical copolymerization of TMPPM, OEGMA, and OEGMA<sub>2</sub> (chemical crosslinking agent), followed by the oxidation of the secondary amine of TMPPM units with H<sub>2</sub>O<sub>2</sub> and Na<sub>2</sub>WO<sub>4</sub> in methanol<sup>[16]</sup> to obtain the P(TEMPO-*r*-OEGMA) hydrogel. Different molar ratios of TMPPM/(TMPPM+OEGMA) (abbreviated as  $X_{TEMPO}$  in the following) were investigated ( $X_{TEMPO} = 0.1, 0.2, 0.3$ , and 0.4) to investigate the influence of increasing TEMPO content and the cross-linker molar ratio OEGMA<sub>2</sub>/(TMPPM+OEGMA) (abbreviated as  $X_{CL}$  in the following) was set to 0.03. Finally, the nitroxide radical units of TEMPO were oxidized into oxoammonium units (TEMPO<sup>+</sup>) with NaClO in the presence HBF<sub>4</sub> to obtain the oxidized P(TEMPO<sup>+</sup>-*r*-OEGMA) hydrogel.<sup>[19]</sup>

### Supporting Information

Supporting Information is available from the Wiley Online Library or from the author.

## Acknowledgements

M.K. is grateful to the International Relation Offices (ADRI) of UCLouvain and to the Académie de recherche et d'enseignement supérieur ARC BATTAB (14/19-057) for financing her Ph.D. J.F.G. is grateful to the Fondation Louvain through the 2018 Marcel de Merre Price for Nanotechnologies for financing this research. E.V.R. is Researcher Qualifié of the Fonds De La Recherche Scientifique. The authors also thank the Joint Lab for Structural Research at the Integrative Research Institute for the Sciences (IRIS Adlershof).

## Conflict of Interest

The authors declare no conflict of interest.

## Keywords

hydrogels, redox responsive hydrogels, rheology, temperature responsive hydrogels, TEMPO

Received: December 11, 2019

Revised: January 21, 2020

Published online:

- 
- [1] N. Chirani, L. H. Yahia, L. Gritsch, F. L. Motta, C. G. Natta, *J. Biomed. Sci.* **2015**, 4, 1.  
[2] I. Willner, *Acc. Chem. Res.* **2017**, 50, 657.

- [3] M. Avais, S. Chattopadhyay, *Polymer* **2019**, 180, 121701.  
[4] L. Tang, L. Gong, G. Zhou, L. Liu, D. Zhang, J. Tang, J. Zheng, *Polymer* **2019**, 173, 182.  
[5] T. Xiang, T. Lu, W. F. Zhao, C. S. Zhao, *Langmuir* **2019**, 35, 1146.  
[6] Z. Sun, Z. Li, Y. He, R. Shen, L. Deng, M. Yang, Y. Liang, Y. Zhang, *J. Am. Chem. Soc.* **2013**, 135, 13379.  
[7] Y. K. Li, C. G. Guo, L. Wang, Y. Xu, C. Y. Liu, C. Q. Wang, *RSC Adv.* **2014**, 4, 55133.  
[8] N. Sun, P. Sun, A. Wu, X. Qiao, F. Lu, L. Zheng, *Soft Matter* **2018**, 14, 4327.  
[9] X. Feng, K. Zhang, P. Chen, X. Sui, M. A. Hempenius, B. Liedberg, G. J. Vancso, *Macromol. Rapid Commun.* **2016**, 37, 1939.  
[10] J. P. Blinco, J. L. Hodgson, B. J. Morrow, J. R. Walker, G. D. Will, M. L. Coote, S. E. Bottle, *J. Org. Chem.* **2008**, 73, 6763.  
[11] A. García-Peñas, C. S. Biswas, W. Liang, Y. Wang, P. Yang, F. J. Stadler, *Polymer* **2019**, 11, 991.  
[12] M. Khodeir, B. Ernould, J. Brassinne, S. Ghiassinejad, H. Jia, S. Antoun, C. Friebe, U. S. Schubert, Z. Kochovski, Y. Lu, E. Van Ruymbeke, J.-F. Gohy, *Soft Matter* **2019**, 15, 6418.  
[13] J. F. Lutz, *J. Polym. Sci., Part A: Polym. Chem.* **2008**, 46, 3459.  
[14] T. Ise, K. Nagaoka, M. Osa, T. Yoshizaki, *Polym. J.* **2011**, 43, 164.  
[15] P. J. Roth, F. D. Jochum, F. R. Forst, R. Zentel, P. Theato, *Macromolecules* **2010**, 43, 4638.  
[16] O. Bertrand, A. Vlad, R. Hoogenboom, J.-F. Gohy, *Polym. Chem.* **2016**, 7, 1088.  
[17] N. Isobe, X. Chen, U. J. Kim, S. Kimura, M. Wada, T. Saito, A. Isogai, *J. Hazard. Mater.* **2013**, 260, 195.  
[18] Q. Fu, A. Sutherland, E. Gustafsson, M. M. Ali, L. Soleymani, R. Pelton, *Langmuir* **2017**, 33, 7854.  
[19] J. M. Bobbitt, *J. Org. Chem.* **1998**, 63, 9367.